Title
Dynamic Response of a Model Levee on Sherman Island Peat: A Curated Data Set

Journal
Earthquake Spectra, 30(2)

ISSN
8755-2930

Authors
Reinert, Edward
Stewart, Jonathan P
Moss, Robb ES
et al.

Publication Date
2014-05-01

DOI
10.1193/101913eqs274m

Peer reviewed

http://dx.doi.org/10.1193/101913EQS274M

Dynamic Response of a Model Levee on Sherman Island Peat: A Curated Dataset

Edward Reinert[a] S.M.EERI, Jonathan P. Stewart,[a] M.EERI, Robb E.S. Moss,[b] M.EERI, Scott J. Brandenberg,[a] M.EERI.

A model levee resting atop soft compressible peaty organic soil in the Sacramento/San Joaquin Delta was shaken by forced vibration to study the seismic deformation potential of the underlying peat and measure dynamic levee-peat interaction. Forced vibration testing occurred over a frequency range of 0 to 5 Hz and produced force amplitudes applied to the embankment crest that induced elastic to nonlinear levee-foundation responses. Available data include acceleration records from sensors mounted on the model levee and on the ground surface near the model levee, and acceleration and pore pressure measurements from sensors embedded in the underlying peat. A remote data acquisition system measured settlements and pore pressures over a span of more than a year, encompassing time before and after the dynamic testing. Small pore pressures were generated in the peat during testing although embankment settlements from cyclic loading were small.

INTRODUCTION

The Sacramento-San Joaquin Delta is a 3,400 km^2 (1,300 mi^2) estuary located at the confluence of the Sacramento and the San Joaquin rivers in California. The Delta is the hub of California's water distribution system, serving over 22 million people in central and southern California and the bay area. Delta levees circumscribe "islands" that are commonly 3-5 m below sea level due to subsidence from oxidation and wind erosion of peaty organic soil that has occurred over the last 150 years (Mount and Twiss 2005). Many of these levees are typically composed of unengineered fill, often loose saturated sand susceptible to liquefaction, and are typically founded on soft peaty organic soils. Seismic stability of Delta levees has recently attracted significant attention (Delta Risk Management Strategy, DRMS 2009, Lund

[a] University of California, Los Angeles, Department of Civil and Environmental Engineering, 5731 Boelter Hall, Los Angeles, CA 90095-1593
[b] Cal Poly State University, San Luis Obispo, Department of Civil and Environmental Engineering, Building 13-217, San Luis Obispo, CA 93407-0353

et al. 2007), and is a central issue in the State's plans to secure its water supply. A major concern is that an earthquake could cause multiple simultaneous levee breaches, drawing saline water from the west into the flooding islands thereby halting water delivery at a direct cost in the tens of billions of dollars (DRMS, 2009). Furthermore, DRMS (2009) and Mount and Twiss (2005) indicate that future seismic events, coupled with rising sea levels and continued subsidence of the islands, will lead to increasingly longer times for saline water to flush out of the Delta, slowing recovery.

A significant driver of seismic risk in the Delta is liquefaction of levee fills, which are saturated because the levees constantly impound water, unlike most flood control levees that are only wet during a flood. Liquefiable cohesionless mineral soil deposits are also sometimes present in the foundation soils beneath the levees, and also contribute to liquefaction hazard. Well established engineering evaluation procedures can be used to evaluate liquefaction-related hazards. Much less is known about the seismic deformation potential of the peat soil underlying many Delta levees. According to ASTM D4427 "Classification of Peat Samples by Laboratory Testing", a soil is classified as "peat" only if the organic content is higher than 75%; a condition not satisfied by much of the organic soil encountered at the test site, which has organic contents ranging from 43 to 64%. We nevertheless refer to the highly organic soil as "peat" in this paper based on local convention, and because most geologists or geotechnical engineers would call this soil "peat" based on visual classification. Researchers have evaluated the modulus reduction and damping behavior of peat (e.g., Wehling et al. 2003, Kishida et al. 2009a) and studied site effects on ground motions for Delta levee cross sections (Kishida et al. 2009b). However, other effects such as cyclic pore pressure generation and related strength loss and volume change have only recently been studied at laboratory scale (Shafiee et al., 2013). Field performance data is generally lacking, with the exception of a few case histories from Japan of poor performance of levees on peat and liquefiable sands (e.g., Sasaki 2009).

Accordingly, as part of a broader effort to investigate potential deformation mechanisms of levees founded on peat, a series of forced-vibration field tests were performed on a model levee constructed atop soft, compressible free-field peat on Sherman Island in the Delta. The purpose of this paper is to describe the data set that was collected from the field tests, including the results of geotechnical and geophysical site investigations, construction of the model levee, long-term monitoring of settlement and pore pressure dissipation, the sequence of force-histories imposed on the model, and the work that was performed to archive the data on

NEEShub. We focus on explaining the data in a manner such that they might be useful to the earthquake engineering community, and interpretation of the test data is reserved for future publications.

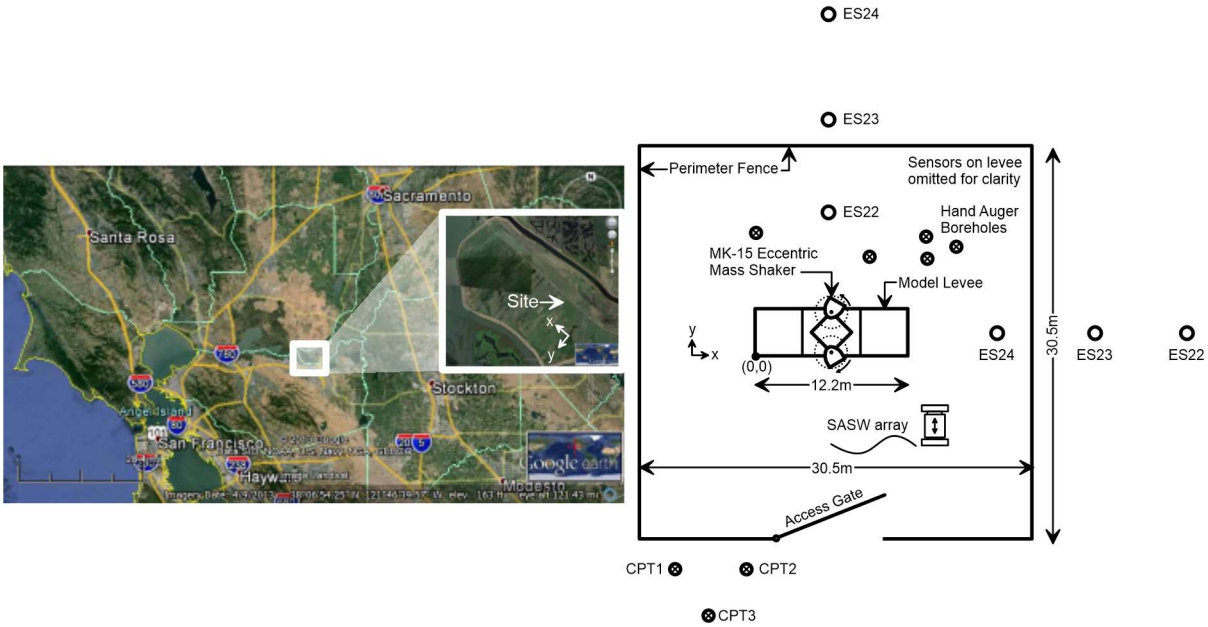

Figure 1. Site plan and map showing location of Sherman Island test site.

SITE INVESTIGATION

Site investigations included geophysical testing for seismic velocities, hand augering and sample retrieval, and cone penetration testing (CPT) at locations specified in Fig. 1. As shown in Fig. 2, these data indicate that the site consists of a 2 m thick desiccated crust of organic soil and peat underlain by 9 m of very soft compressible saturated peat, which in turn is underlain by sand. The organic content of the peat was high from depths of 2 m to about 6 m, and more inorganic clay minerals were encountered in the peat below about 6 m although the peat was still primarily composed of organic material. At the time of testing in 2011, the natural ground water level was approximately 2 m below the ground surface, although the water level was raised modestly for subsequent testing in 2012.

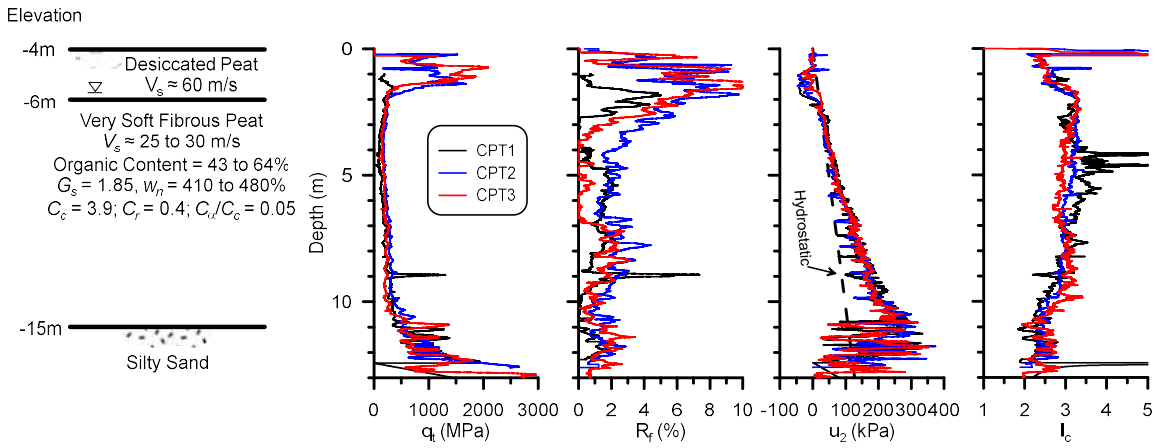

Figure 2. Cone penetration test data and interpreted geotechnical profile from Sherman Island site.

Geophysical testing at the site employed surface wave and downhole tests (the downhole measurements used a geophone in the CPT). In the surface wave tests, we deployed linear arrays of accelerometers and an impact source, and we also used passive surface wave tests recording ambient vibrations. Rayleigh wave phase velocities ranged from 27 to 31 m/s (average=29 m/s) for a wavelength range of 2 to 5 m, which encompasses the depths of the soft saturated peaty foundation soils. Rayleigh wave velocity was as high as 57 m/s at wavelengths shorter than 2 m in the desiccated crust. We do not show a shear wave velocity profile inverted from the Rayleigh wave dispersion curve because the stiff crust overlying the soft peat results in a multi-modal response that complicates surface wave interpretation. Downhole testing in the peat indicates shear wave velocities in the range of 25-30 m/s, which is generally consistent with the surface wave tests. Further analysis of the data, given in Reinert et al. (2013), indicates that the small strain material damping is in the range of 2 to 4% and that the natural frequency of the peat layer is about 3 Hz. This natural frequency is consistent with propagation of a first-mode Rayleigh wave with wavelength equal to the deposit thickness ($f_1 = V_r/\lambda$ = 30 m/s / 11 m).

Hand auguring occurred in June and August 2011, during which we retrieved piston samples for laboratory testing and performed in situ vane shear tests. A slurry was not utilized to support the boreholes, which began to squeeze shut below a depth of 2 m. However, we found that the peat materials were sufficiently soft to allow manual advancement of a closed-ended piston sampler from the bottom of the 2 m deep borehole to the desired sample depth in peat. When the sampler reached the desired depth, the piston was unlocked and the sampler was advanced into the materials to be sampled. Water was poured on top of the piston to form a vacuum seal, and the sample was subsequently retrieved from the borehole. Using this

configuration, it was possible to retrieve relatively undisturbed samples from depths as great as 6 m, and full recovery was obtained for every sample. Truly "undisturbed" samples of peat cannot be obtained because the peat is relatively free-draining (water can be squeezed out by hand compressing the peat), and the fibers must be cut as the sampler is advanced. Wehling et al. (2003) found that effects of disturbance on Shelby tube samples of Sherman Island peat is relatively small, and we believe our samples are suitable for laboratory strength and deformation testing.

Laboratory testing of samples collected during the site investigation is described by Stewart et al. (2013). The data indicate that the organic content of the peat ranged from 43 to 64%, natural water content ranged from 410 to 480%, and the specific gravity of the solids is G_s = 1.8. Additional information on consolidation, secondary compression, and soil behavior under cyclic shearing conditions is given in Stewart et al. (2013).

Three cone penetration test soundings performed at the site in September 2012 are shown in Figure 2. The data confirm that the peat is extremely soft (the CPT rod had to be held up with pipe wrenches to prevent it from penetrating under its self-weight into the peat when the grip was released to raise the hydraulic press). The soil behavior type (SBT) for the peat below a depth of 2m was generally in the "Sensitive fine-grained", "Clay – organic soil", and "Clays: clay to silty clay" regions based on the Robertson (2010) normalized SBT chart. Dissipation tests performed in the peat indicated that the time required for dissipation of 50% of the excess pore pressure (i.e., t_{50}) ranged from about 1 to 2 minutes, indicating the range of hydraulic conductivity of the peat is about 10^{-7} to 10^{-5} cm/s following the procedure given in Robertson et al. (1992). These measurements reflect horizontal hydraulic conductivity, which is expected to be much higher than vertical (e.g., Mesri and Ajlouni 2007).

Dissipation tests performed in the sand below the peat identified artesian conditions at the site, with steady-state pore pressures near 150 kPa at the top of the sand compared with 90 kPa that would correspond to hydrostatic conditions. Artesian pressures are anticipated because the sand is hydraulically connected to the adjacent river, and the surface of Sherman Island is approximately 4m below river level (sea level in this case). Artesian pressures have been observed by others, and contribute to an ever-increasing fraction of agricultural land in the Delta being too wet to farm (e.g., Deverel and Hart 2012). Based on the measured artesian pressures, and measured total unit weights, our interpretation is that the effective stress at the

sand/peat interface is approximately zero. This artesian condition must be accounted for in the interpretation of effective stresses at the site.

SPECIMEN CONSTRUCTION AND INSTRUMENTATION

Construction of the test specimen began by clearing vegetation from the site, and installing subsurface piezometers. Four KPSI 330 piezometers were manually pushed through open boreholes into the soft peat below the water table with a steel mandrel. The tips of the piezometers were covered in fabric to prevent migration of soil solids into the sensor, and the sensor was permitted to become saturated in water in the borehole prior to pushing them into the peat. The inside of the transducers is sealed, making them sensitive to atmospheric pressure fluctuations. Hence, a fifth piezometer was placed on the ground surface to monitor atmospheric changes that were subsequently subtracted from the subsurface piezometer readings to render gauge pressure measurements.

After installing the piezometers, we hand augured boreholes that were subsequently cased with PVC pipe where the subsurface accelerometers would be placed prior to dynamic testing (Fig. 3). An in-place inclinometer consisting of 40 bi-axial micro-electro-mechanical system (MEMS) accelerometer sensors spaced 0.30 m apart was placed horizontally along the center axis of the specimen. The inclinometers consisted of five INC500 modules manufactured by Geodaq, Inc., and permitted measurements of specimen settlement. The piezometers and inclinometer were remotely monitored at 10 minute intervals (except just after construction and during dynamic testing; see Remote Monitoring Data section below) and data were communicated to a website maintained by Geodaq.

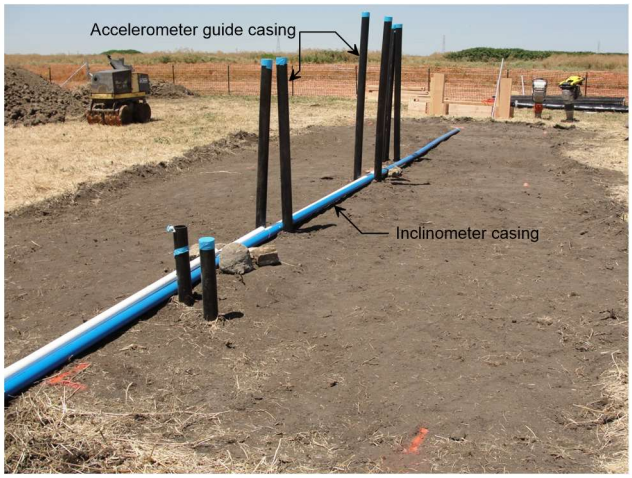

Figure 3. Test site prior to construction of test specimen showing horizontal inclinometer casing and vertical accelerometer guide casings.

The model levee was engineered to transmit the energy from the shaker downward into the underlying peat. This required the use of geosynthetic reinforcement and compaction of the clay fill, rendering the model levee stronger than typical Delta levees composed of unengineered earth fill that is often susceptible to liquefaction. The embankment was constructed by first placing a thin layer of fill to cover the inclinometer casing, and subsequently unrolling Tencate 2XT biaxial geogrid and Mirafi 500x woven geofabric in the transverse direction (i.e., left-to-right in Fig. 3). The geogrids and geofabric were wrapped in the out-of-plane direction in order to form vertical faces at the edge of the embankment, and were supported during construction using pre-fabricated falsework. Sandy clay fill was then placed atop the geogrid and compacted using hand-operated equipment to dry unit weights ranging from 15.9 to 17.6 kN/m^3 (16.8 kN/m^3 average) at water contents ranging from 5.5 to 10.4%. The modified Proctor (ASTM 1980) maximum dry density is 19.4 kN/m^3 and optimum water content is 11%. The specimen was constructed in six lifts, each of which was approximately 0.3 m thick. A sturdy timber frame was placed after construction of the third lift, and soil was compacted around and inside the frame, thereby connecting it to the specimen. The MK-15 shaker was mounted on a deck constructed atop the embedded frame. Figure 4 is a photo of the test specimen, which was 1.8 m tall, 12.2 m long (left-to-right in Fig. 4), and 3.7 m wide. The side-slopes were constructed at a 2:1 angle, and the crest width was 5.0 m.

Figure 4. MK-15 eccentric mass shaker mounted atop test specimen.

Testing of the specimen occurred in two stages, which were in 2011 and 2012. During these tests, the model levee essentially performed as designed, and did not exhibit large permanent

deformations in response to imposed shaking. The good performance of the model levee is not relevant to seismic performance of Delta levee fills, as our focus was on the seismic performance of the underlying peat rather than the levee fill.

Figures 5 and 6 show sensor layouts for both phases of testing. The in-ground MEMS accelerometers (M1-M8) were placed first, prior to the attachment of the deck and the MK15 shaker. The triaxial MEMS accelerometers were sealed in PVC tubes with epoxy and pushed into the soil through the PVC casings into the peat, while carefully maintaining the alignment of the sensors. A thin steel cable attached to the sensors enabled them to be pulled out of the ground after testing. The above-ground accelerometers consisted of 25 triaxial accelerometers (either Episensor Triaxial accelerometers or mounted sets of three Episensor uniaxial accelerometers that acted as a single triaxial accelerometer) placed on the embankment and in the free field, as well as a single uniaxial accelerometer mounted on the embankment. Accelerometers were attached to the sides of the embankment using steel plates that were pushed between the geogrid-reinforced lifts. In addition to the sensors mounted on the specimen, two surface arrays of triaxial accelerometers were oriented in the X- and Y-directions as seen in Fig. 1, and a sensor, ES26, was placed as far away from the embankment as our sensor cables would permit to record attenuation of shaking amplitude with distance and to assess potential vibrations of existing levees along the San Joaquin River and Mayberry Slough. An additional accelerometer was placed at the nearest levee location, and was set to trigger at a low acceleration level to indicate whether our testing activities were mobilizing measureable shaking levels at the levees. This sensor never triggered as a result of our testing.

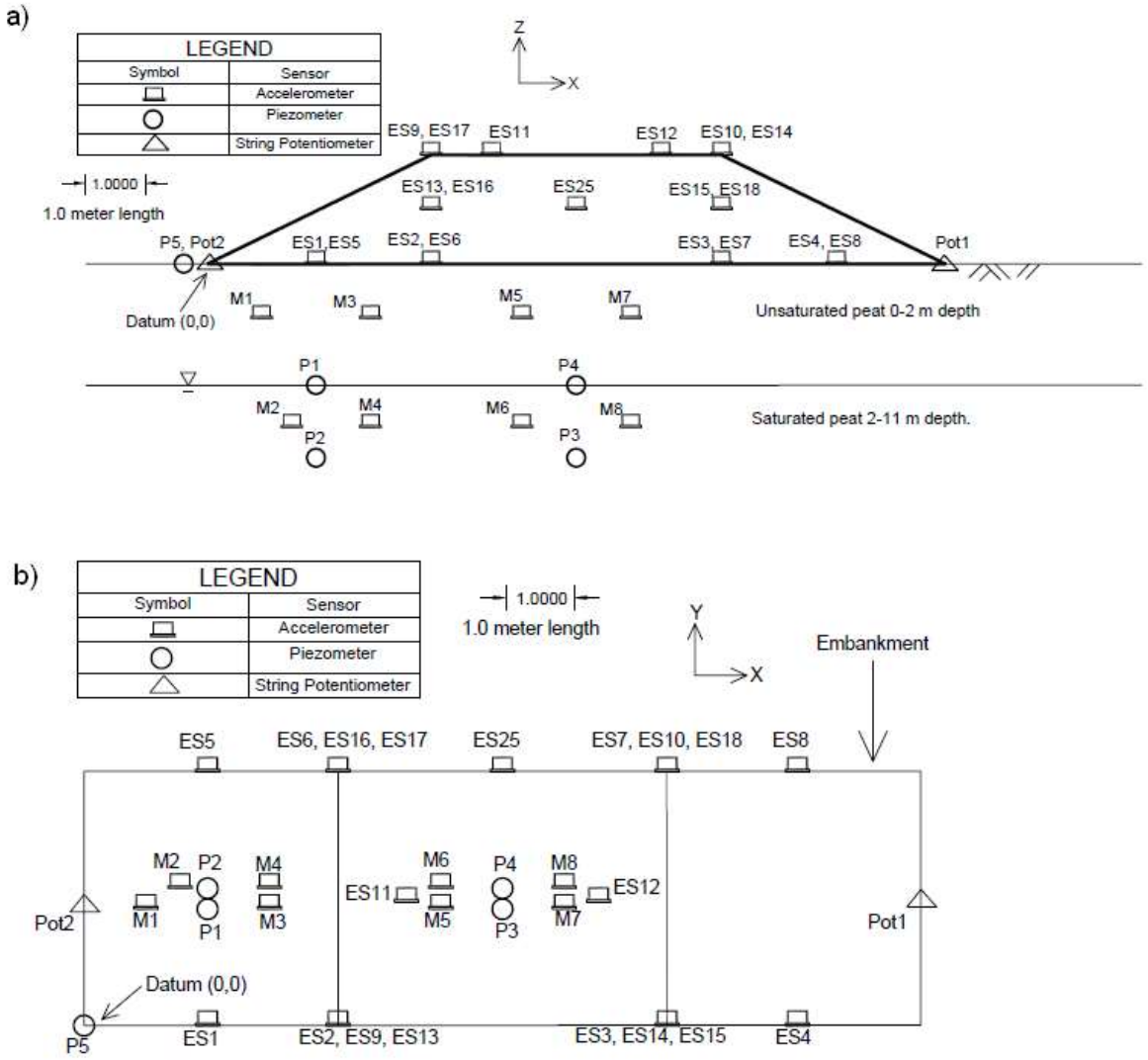

Figure 5. (a) Elevation and (b) plan view of the sensor layout used in the 2011 test. Shaker sketch omitted for clarity.

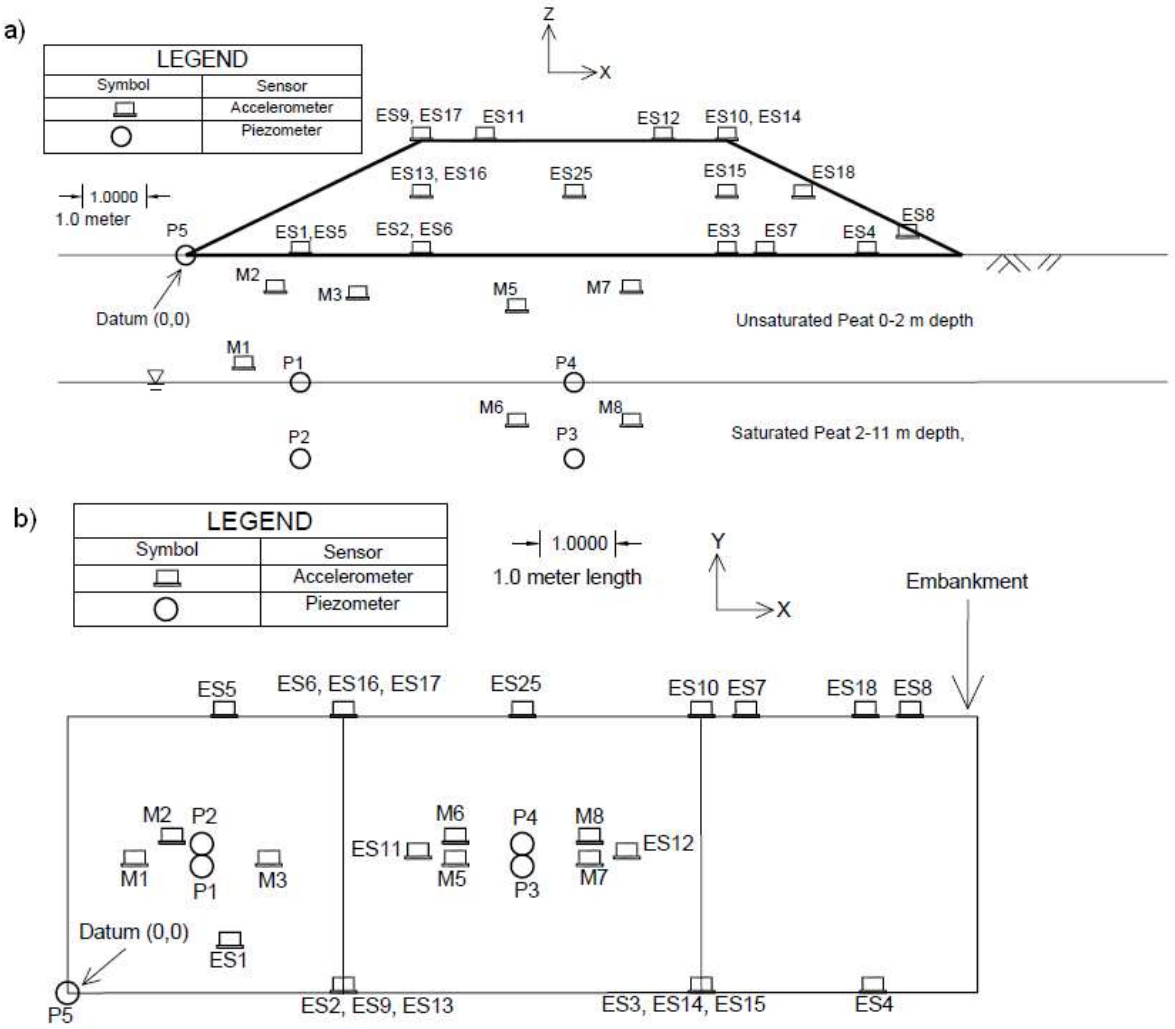

Figure 6. (a) Elevation and (b) plan view of the sensor layout used during the 2012 test. Shaker sketch omitted for clarity.

Several changes to the specimen were made for the 2012 test:

- Because the testing in 2011 formed a gap between the shaker frame and the compacted fill, the upper three lifts were reconstructed for the 2012 test. Timber feet were added to the bottom of the frame to improve coupling with the embankment soil.
- Because the natural groundwater depth of 2 m is not representative of actual levees (whose foundations are saturated over their full thickness), we constructed a berm around the embankment and flooded the local region by pumping in water from a nearby drainage ditch.
- A triaxial accelerometer (ES19A) was added next to sensor ES19, which was faulty. Data from both sensors are included in the NEEShub dataset.

- The placement of the MEMS accelerometers was changed. Accelerometer M4 could not be retrieved following the 2011 tests. Some of the MEMS sensors were shallower in 2012, due to stiffening of the peat that prohibited manual pushing of the sensors.

FORCED VIBRATION TEST DATA

The test data archived on NEEShub is organized into Experiments, Trials, and Repetitions in conformance with NEEShub data archiving standards, as summarized in Table 1. Seven of the experiments are curated and have been issued digital object identifiers (DOI's). Experiments 3 through 6 were collected during the 2011 test, and Experiments 7 through 9 were collected during the 2012 test. Each of these tests has an Experiment corresponding to the MK-15 shaker testing, an Experiment for SASW testing, and an Experiment containing continuous raw data files. The 2011 test has an additional experiment corresponding to Atom Ant testing (the Atom Ant shaker was unavailable during the 2012 test). We believe that Experiments 3 and 7, corresponding to the MK-15 shaker tests, are the most useful for potential users of our data set. Experiment 2 contains a report summarizing the geophysical study conducted in March 2010, results of which are summarized in the data report.

Table 1. Summary of Experiments, Trials, and Repetitions archived on NEEShub.

Experiment	Number of Trials	Number of Repetitions	DOI
2: Geophysical Study	0	0	N/A
3: Field Testing with MK-15 Shaker	6	19	10.4231/D3SF2MB89
4: SASW Array	4	14	10.4231/D3J09W43H
5: Shaker Testing with Atom Ant Shaker	2	7	10.4231/D3D795994
6: Continuous Raw Data Files	4	4	10.4231/D34Q7QQ2B
7: Field Testing with MK-15 Shaker (2012 Re-Test)	6	23	10.4231/D38G8FH6G
8: SASW Array (2012 Re-Test)	2	6	10.4231/D30Z70W8Z
9: Continuous Raw Data Files (2012 Re-Test)	1	1	10.4231/D3NP1WJ45

We focus specifically on data collected during Experiments 3 and 7 in this paper; details for other experiments are given in the data report (Reinert et al. 2013). Three different functions of frequency versus time were imposed on the shaker, as shown in Fig. 7 and described below:

1. Frequency sweeps consisted of shaking the embankment at increasing frequency until a target frequency was reached, and subsequently spinning back down to zero

frequency. Test durations were either fast (100-120 seconds) or slow (300-360 seconds).

2. Step sweeps consisted of shaking at a single frequency for a fixed period of time, which is repeated at multiple frequencies. Typically, the frequency step between intervals was 0.5 Hz. The duration of shaking at each step was normally about 10 seconds.

3. Dwell sweeps are similar to frequency sweeps, except that the shaking is sustained at a given target frequency for the main body of the test.

Tables 2 and 3 summarize the sequences of motions imposed on the specimen by the MK-15 shaker for the 2011 and 2012 tests. The force imposed in the x-direction by the shaker at its point of connection to the timber frame, F_x, is given as:

$$F_x = \left(m_b + m_r\right) a_{b,x} + m_r r \omega^2 \cos\theta \quad (1)$$

where m_b is the mass of the shaker frame excluding the rotating baskets, m_r is the mass of the rotating baskets, $a_{b,x}$ is the acceleration of the center of mass of the shaker, r is the radius from the center of rotation to the center of mass of the rotating basket, ω is the angular frequency of the baskets, and θ is the position of the baskets ($\theta = 0$ when the line from the spindle through the center of mass is aligned in the x-direction).

The shaker forcing function computed using Eq. 1 is included in the corrected data files for Experiments 3 and 7. Details of these calculations are described by Reinert et al. (2012), and are omitted here for brevity.

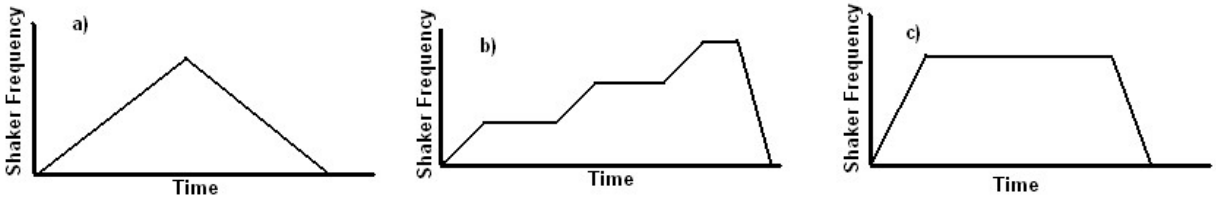

Figure 7: Schematic representation of shaker frequency for a) frequency sweep, b) step sweep, c) dwell sweep.

Table 2: 2011 MK15 Test sequence

Trial	Repetition	Date	Repetition Start Time PDT (Approx)	Repetition Duration (s)	Frequency Function	Shaker Eccentricity, $m_r r$ (Mg-m)
1	1	8/27/2011	14:50:00	80	Step Sweep	0.059
1	2	8/27/2011	15:07:00	80	Step Sweep	
1	3	8/28/2011	11:49:00	360	Frequency Sweep	
1	4	8/28/2011	12:00:30	120	Frequency Sweep	
1	5	8/28/2011	12:05:30	115	Step Sweep	
1	6	8/28/2011	12:09:30	180	Dwell Sweep	
2	1	8/28/2011	12:51:30	360	Frequency Sweep	0.126
2	2	8/28/2011	13:05:30	120	Frequency Sweep	
2	3	8/28/2011	13:10:30	100	Step Sweep	
2	4	8/28/2011	13:14:30	180	Dwell Sweep	
3	1	8/29/2011	9:47:30	360	Frequency Sweep	0.251
3	2	8/29/2011	9:57:30	120	Frequency Sweep	
3	3	8/29/2011	10:04:30	125	Step Sweep	
3	4	8/29/2011	10:08:30	180	Dwell Sweep	
4	1	8/29/2011	10:57:30	120	Frequency Sweep	0.362
4	2	8/29/2011	11:32:30	360	Frequency Sweep	
5	1	8/29/2011	14:04:30	120	Frequency Sweep	0.517
5	2	8/29/2011	14:17:30	120	Frequency Sweep	
5	3	8/29/2011	14:31:30	120	Frequency Sweep	

Table 3: 2012 MK15 test sequence

Trial	Repetition	Date	Repetition Start Time PDT (Approx)	Repetition Duration (s)	Frequency Function	Eccentricity Constant, $m_r r$ (Mg-m)
1	1	8/14/2012	14:10:00	360	Frequency Sweep	0.059
1	2	8/14/2012	14:31:00	120	Frequency Sweep	
1	3	8/14/2012	14:38:00	100	Step Sweep	
1	4	8/14/2012	14:43:00	180	Dwell Sweep	
2	1	8/14/2012	15:23:00	360	Frequency Sweep	0.126
2	2	8/14/2012	15:32:00	120	Frequency Sweep	
2	3	8/14/2012	15:36:00	100	Step Sweep	
2	4	8/14/2012	15:39:00	180	Dwell Sweep	
3	1	8/15/2012	11:01:00	360	Frequency Sweep	0.251
3	2	8/15/2012	11:10:00	360	Frequency Sweep	
3	3	8/15/2012	11:18:00	120	Frequency Sweep	
3	4	8/15/2012	11:22:00	100	Step Sweep	
3	5	8/15/2012	11:25:00	180	Dwell Sweep	
4	1	8/15/2012	12:03:00	360	Frequency Sweep	0.362
4	2	8/15/2012	12:10:00	360	Frequency Sweep	
4	3	8/15/2012	12:33:00	120	Frequency Sweep	
4	4	8/15/2012	12:43:00	85	Step Sweep	
5	1	8/15/2012	13:16:00	120	Frequency Sweep	0.517
5	2	8/15/2012	13:23:00	360	Frequency Sweep	
5	3	8/15/2012	13:43:00	150	Step Sweep	
5	4	8/15/202	13:54:00	120	Frequency Sweep	
6	1	8/15/2012	15:44:00	120	Frequency Sweep	0.568
6	2	8/15/2012	15:52:00	180	Dwell Sweep	

DATA ACQUISITION AND PROCESSING

All of the experimental data except for a few sensors required to measure the shaker forcing function were acquired using a Rockhound data acquisition system consisting of fifteen Kinemetrics Q330 data loggers that each recorded six channels of data and two Kinemetrics Granite data loggers each recording 12 channels of data (114 channels in total). Each data acquisition system shares a common timestamp via GPS clock synchronization. The sampling frequency was 200 Hz for data collected using this system. A National Instruments system was used to record data from two rotary encoders that measure the position and frequency of the shaker baskets, and horizontal acceleration of the shaker frame from one accelerometer. A sampling frequency of 2,000 Hz was used to record these data. Data from the two systems were time-synchronized using cross-correlation of the horizontal acceleration of the shaker frame, which was measured using both systems. The Rockhound system continuously sampled data, and hour-long blocks of the raw data were saved into three files; one file for the Q330 system and one for each Granite systems. These blocks of raw data are uploaded to the NEEShub data repository because users might potentially be interested in ambient vibrations, or other features of the recorded data that do not correspond to a particular shaking event. The National Instruments system was manually triggered prior to each repetition, therefore these data are not archived in the hour long blocks.

The start time for each test (referred to as a 'repetition') was recorded in a log book, and snippets of data corresponding to each repetition were extracted from the hour-long blocks of data using an algorithm (snippet.exe) uploaded to the NEEShub data repository. The data saved for a repetition includes 5 to 10 seconds of ambient vibrations before and after active shaking. The snippets of data from the Granite and Q330 systems were subsequently combined into a single data file and uploaded as Unprocessed Data for each repetition. The unprocessed data are stored in units of bit counts, and can be converted to volts by dividing by 2^{24} and multiplying by 40 volts, which is the peak-to-peak range of the A/D converter.

The Converted Data files were derived from Unprocessed Data files by modifying the signals to engineering units (including necessary coordinate transformations for proper sign convention) and re-arranging into an order that corresponds to the sensor ID's. The Converted Data files have a first column containing the time vector, followed by on-ground accelerometers in order of sensor ID, followed by subsurface MEMS accelerometers in order

of sensor ID, followed by the command frequency for the MK15 shaker, and finally the pore pressure transducers in order of sensor ID.

Corrected Data were obtained from the Converted Data files by applying baseline corrections, which consist of subtracting the mean value from acceleration records and offsetting piezometer records to accurately reflect initial steady-state pore pressures. These offsets are required because voltage zero does not always correspond to physical zero. The corrected data are not high-pass filtered, which is required to avoid drift and unrealistic features in velocity and displacement histories due to noise. Finally, Derived Data were obtained from the Corrected Data files by computing the shaker forcing function following the procedure described by Reinert et al. (2012), and appending the shaker forcing function to the end of each data column.

SAMPLE DATA

In this section we present samples of data collected during the experiments. The purpose of showing the data is to illustrate data quality, and to provide a reference to aid users of our data who wish to verify that they are correctly plotting and interpreting the data files from NEEShub. Although our intent is not to derive engineering conclusions, we will identify obvious features in the plots. Figure 8 shows horizontal acceleration in the *x*-direction at the top and bottom of the model levee and in the underlying peat at depths of 0.9 m and 2.7 m. These records are for Experiment 3, Trial 2, Repetition 2, in which a sweep function was imposed by the MK-15 shaker. The maximum frequency was 3Hz, and the shaker reached this frequency at 64 s. The acceleration records exhibit a characteristic shape in which the amplitude increases as frequency increases. Accelerations are largest at the crest of the levee, with a peak of 0.11 g, and amplitude decreases with depth. The lack of symmetry in the acceleration histories was caused by pounding between the shaker frame and the levee fill. The decrease in acceleration amplitude with depth is influenced by the top-down shaking condition imposed by forced vibration testing.

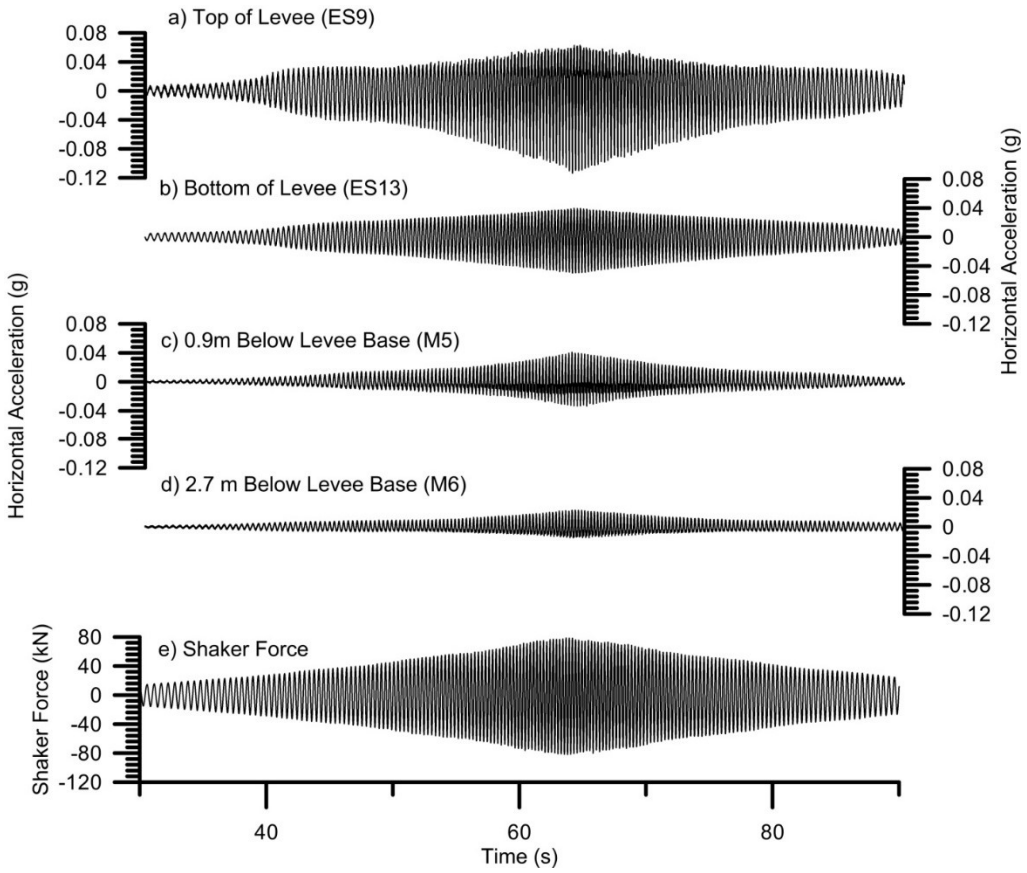

Figure 8: Horizontal acceleration recorded at various depths for sweep function during Experiment 3, Trial 2, Repetition 2.

Figure 9 shows vertical-component ground accelerations at various distances from the embankment in the *x*-direction. These records are for Experiment 3, Trial 4, Repetition 1, in which a large-amplitude sweep function was applied by the MK-15 shaker. The maximum frequency of 3 Hz was reached at approximately 48 s. The largest acceleration was recorded at the embankment toe, and acceleration amplitude decreased with distance from the model levee. The ground surface motions recorded in the free-field are likely dominated by Rayleigh waves, and these data can be used to develop the low-frequency portion of the Rayleigh wave dispersion curve. Attenuation of the waves with distance results from both geometric spreading of the wavefronts and material damping.

Figure 10 shows a pore pressure record obtained in the peat beneath the levee at a depth of 3.2 m during a sweep function from Experiment 3, Trial 4, Repetition 1. The pore pressures exhibit dynamic responses, which indicate that the sensors were responsive to the dynamic conditions during shaking, in turn suggesting the sensors were well-saturated. Unsaturated piezometers exhibit poor high frequency response due to the compressibility of the gas in contact with the transducer. In addition to the dynamic response, the pore pressures slowly

increase during shaking by nearly 0.3 kPa from the beginning to the end of the test. Interestingly, pore pressures continue to increase after shaking ends. These small increases in pore pressure are smaller than the long-term fluctuations that are associated with pumping operations to control the groundwater level on Sherman Island. However, the shaking events occur during much shorter time scales compared with groundwater fluctuations, and pore pressure increases were repeatable for the large intensity events. These observations indicate that the pore pressures were caused by shearing induced by shaking, and not by fluctuations in ground water level.

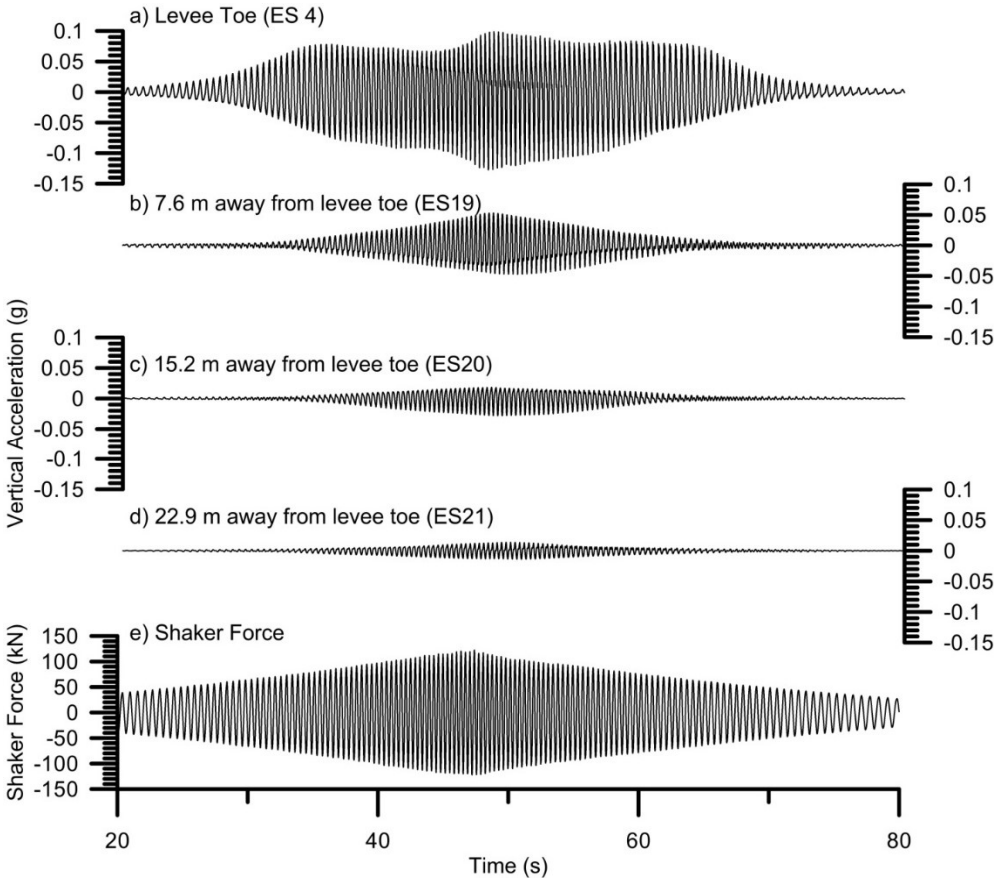

Figure 9: Vertical acceleration recorded on surface at various distances for sweep function during Experiment 3, Trial 4, Repetition 1.

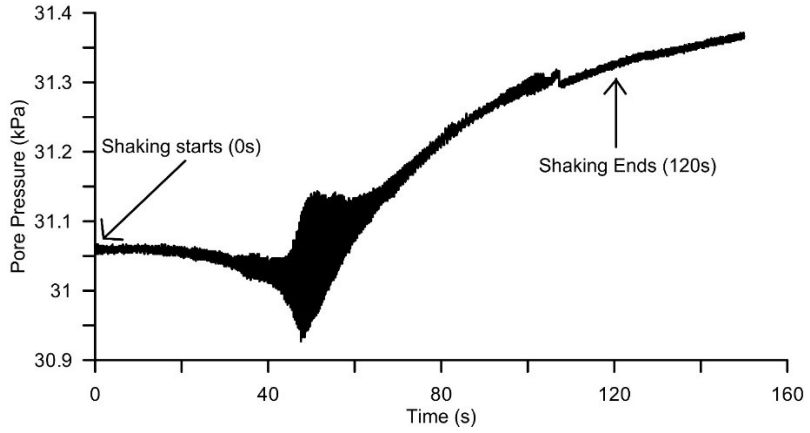

Figure 10: Pore pressure recorded in the peat at a depth of 3.2 m from sensor P3 Experiment 3, Trial 4, Repetition 1.

REMOTE MONITORING DATA

The remote monitoring system collected data from five piezometers and the inclinometer array to evaluate pore pressures and embankment settlement (Reinert et al. 2013). The system generally sampled data every ten minutes, although more frequent sampling intervals were used immediately after construction. The inclinometer was always connected to the remote data acquisition system. Piezometers were also connected to this system except during the days of forced vibration testing, during which they were connected to the dynamic data acquisition system. Therefore, two gaps in the piezometer data (from the remote system) correspond to the testing days. Piezometers were immediately re-connected to the remote data acquisition system following testing for post-shake monitoring.

Figure 11 shows pore pressures and settlements beneath the center of the embankment over a period of about 13 months. Data begin at embankment construction, during which pore pressures and settlements rapidly increase as lifts of fill are placed. Excess pore pressures dissipated quickly, and decreased to pre-construction levels after a few days. The pore pressure changes are attributed to dissipation caused by consolidation and fluctuations in groundwater depths (which can change daily from pumping related to regional agricultural operations). Approximately 50 days after the data acquisition began, pore pressures suddenly increased and fluctuated in time. We believe this change was caused by pumping operations, and is unrelated to our test activities. The levee settlement continued to occur at a significant rate even after excess pore pressures had been dissipated. We attribute this to secondary compression of the peat. The settlement rate increased upon local flooding of the peat beneath the levee. The

remote monitoring data indicate that no significant changes in settlement rate or pore pressures were induced by shaking.

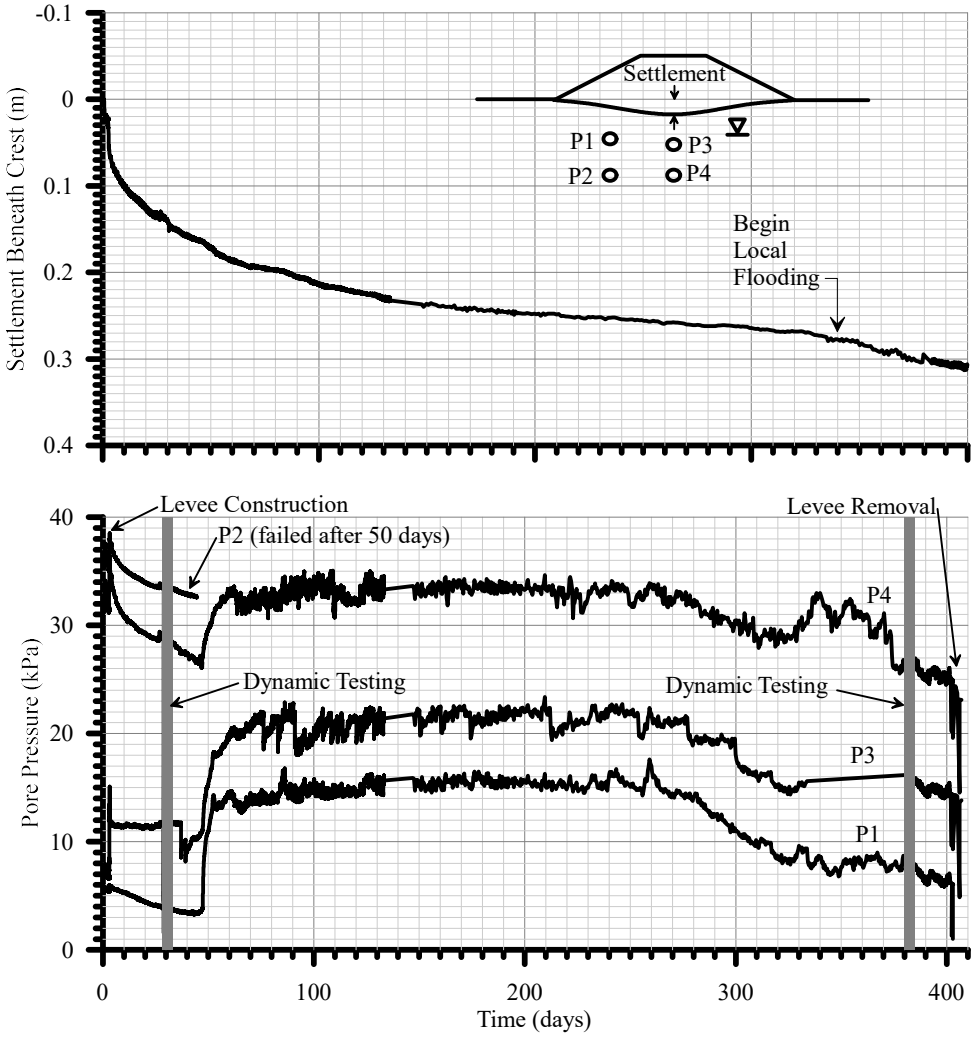

Figure 11. Remote monitoring data on pore pressures and embankment settlement

SUMMARY AND CONCLUSIONS

This data paper presents results from a first-of-its-kind field testing program of a model levee resting atop soft and compressible peaty organic soil in the Sacramento/San Joaquin Delta. The NEES@UCLA MK-15 eccentric mass shaker was mounted on a timber frame embedded in the model levee. Shaking operations imposed significant transient deformations within the model levee and the foundation soil. The test data are archived in the NEEShub data repository; seven experiments have been issued Digital Object Identifiers. This paper presents the instrumentation plan and sample data, and is intended to aid researchers who wish to use our data.

The purpose of these tests was to observe potential seismic deformation mechanisms in the peat that might contribute to levee fragility. The shaking imposed shear strains on the underlying saturated peat that resulted in small, but measurable, increases in excess pore water pressure. This is consistent with laboratory test data showing that cyclic loading of saturated peat can generate excess pore pressures, the subsequent dissipates of which results in settlement. No measurable increase in settlement was observed from these tests because the mobilized excess pore pressures were very small, nevertheless, this test is proof of the concept that cyclic loading can cause increases in excess pore pressure in peat under field conditions. Settlements associated with reconsolidation are not currently included in any seismic levee evaluation procedures, and additional work is needed to clarify this issue.

ACKNOWLEDGMENTS

The authors would like to acknowledge the following people for assistance during the test: Mike Driller, Bryan Brock, Dave Mraz, and Nancy Vogel from the Department of Water Resources, the nees@UCLA group including Bob Nigbor, Steve Keowen, Alberto Salamanca, Sophia Poulos, and Jackson English, and UCLA students Pavlo Chrysovergis, Sean Ahdi, and Ali Shafiee. We also thank John Lemke and GeoDAQ for providing the remote data monitoring system, Linda Leeman and Lisa Kashiwase, Ascent Environmental, for biological monitoring, and Bruce and Roy Gornto, Gornto Ditching, for constructing the embankment. This research was supported by the National Science Foundation under award number 0830081 through the George E. Brown Network for Earthquake Engineering Simulation (NEES) program in coordination with cognizant program official for this grant is Richard J. Fragaszy. Any opinions, findings, and conclusions or recommendations expressed in this material are those of the author(s) and do not necessarily reflect the views of the National Science Foundation. This material is based upon research performed in a renovated collaboratory by the National Science Foundation under Grant No. 0963183, which is an award funded under the American Recovery and Reinvestment Act of 2009 (ARRA).

REFERENCES

ASTM (1980). ”Natural Building Stones: Soil and Rock,” *Annual Book of ASTM Standards,* Part 19, Philadelphia, 634 pp.

Deverel, S., and Hart, C. (2012). “What is the future of farming on organic soils in the Sacramento-San Joaquin Delta.” HydroFocus, Inc. 36 p.

URS Corporation, Jack R. Benjamin and Associates (2009). "Delta Risk Management Strategy (DRMS) Phase I Report." California Department of Water Resources.

Kishida, T., Wehling, T. M., Boulanger, R. W.,Driller, M. W., and Stokoe, K.H. II (2009a). "Dynamic Properties of Highly Organic Soils from Montezuma Slough and Clifton Court”. *J. Geotech. Geoenviron. Eng.,* 135(4), 525-532.

Kishida, T., Boulanger, R., Abrahamson, N., Wehling, T., and Driller, M. (2009b). ”Regression Models for Dynamic Properties of Highly Organic Soils.” *J. Geotech. Geoenviron. Eng.*, 135(4), 533–543.

Lund, J., Hanak, E., Fleenor, W., Howitt, R., Mount, J., and Moyle, P. (2007). "Envisioning futures for the Sacramento-San Juaquin Delta." Public Policy Institute of California. San Francisco, CA, 325 p.

Mesri, G. and Ajlouni, M. (2007). “Engineering properties of fibrous peats.” *J. Geotech. Geoenviron. Eng.*, 133(7): 851-866.

Mount, J.F., and Twiss, R. (2005). "Subsidence, Sea Level Rise, Seismicity in the Sacramento-San Joaquin Delta." San Francisco Estuary and Watershed Science, Vol. 3, Article 5, available at http://repositories.cdlib.org/jmie/sfews/vol3/iss1/art5.

Reinert, E.T., Brandenberg, S.J., Stewart, J.P., Moss, R.E.S. (2012). “Dynamic Field Testing of a Model Levee Founded on Peaty Organic Soil Using an Eccentric Mass Shaker.” Proceedings of the 15th World Congress on Earthquake Engineering, Lisbon, Portugal.

Reinert, E.T., Lemke, J., Stewart, J.P., Brandenberg, S.J. (2013). “Remote Monitoring of a Levee Constructed on Soft Peaty Soil.” Proceedings GeoCongress 2013, San Diego, CA.

Robertson, P.K., Sully, J.P., Woeller, D.J., Lunne, T., Powell, J.J.M., and Gillespie, D.G. (1992). “Estimating the coefficient of consolidation from piezocone tests.” *Canadian Geotechnical Journal*, 29(4), 551-557.

Sasaki, Y. (2009). "River dike failures during the 1993 Kushiro-oki earthquake and the 2003 Tokachi-oki earthquake," Earthquake geotechnical case histories for performance-based design - Kokusho (ed), 2009 Taylor & Francis Group, London, pp. 131-157, 2009.

Shafiee, A., Brandenberg, S.J., and Stewart, J.P. (2013). “Laboratory Investigation of the Pre- and Post-Cyclic Volume Change Properties of Sherman Island Peat.” Proceedings GeoCongress 2013, San Diego, CA.

Stewart, J.P., Brandenberg, S.J., and Shafiee, A. (2013). "Laboratory evaluation of seismic failure mechanisms of levees on peat." UCLA Structural & Geotechnical Engineering Laboratory, Report No. 2013/04. 62 p.

Wehling, T.M., Boulanger, R.W., Arulnathan, R.,Harder, L.F., andDriller, M.W. (2003). "Nonlinear dynamic properties of a fibrous organic soil." *J. Geotech. Geoenviron. Eng.,* 129(10), 929-939.